Asian Journal of Chemistry; Vol. 31, No. 1 (2019), 229-234

ASIAN JOURNAL OF CHEMISTRY

https://doi.org/10.14233/ajchem.2019.21665

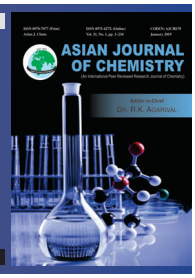

Synthesis and Characterization of Ni/ZrO_2-Bentonite

MOHAMAD MIRZAN[1], KARNA WIJAYA[2,*], IIP IZUL FALAH[2] and WEGA TRISUNARYANTI[2]

[1]Department of Chemistry, Faculty of Mathematics and Natural Sciences, Universitas Tadulako, Palu 94118, Indonesia
[2]Department of Chemistry, Faculty of Mathematics and Natural Sciences, Universitas Gadjah Mada, Yogyakarta 55283, Indonesia

*Corresponding author: E-mail: karnawijaya@ugm.ac.id

Received: 20 August 2018; *Accepted*: 22 October 2018; *Published online*: 30 November 2018; AJC-19186

Bentonite as a carrier was modified by means of pillarization using $ZrOCl_2 \cdot 8H_2O$ pillaring solution. Calcination was performed to obtain ZrO_2 bounded bentonite. To create a bifunctional catalyst, ZrO_2-bentonite was impregnated using $Ni(NO_3)_2 \cdot 6H_2O$ precursor as nickel metal source. Subsequently, calcination and reduction steps were performed to obtain Ni/ZrO_2-bentonite catalyst. The physical-chemical properties of catalyst was characterized by XRD, XRF and the surface area was analyzed with BET, surface acidity with gravimetric method using NH_3 vapour, FT-IR and TEM. The characterized results by XRD showed specific peaks of montmorillonite mineral still visible after the pillarization and impregnation process with nickel metal. The XRD analysis also showed an increase in basal spacing d_{001} of the catalyst sample after the pillarization process characterized by the shifting of specific peaks d_{001} to the left ($2\theta < 5°$). The XRF analysis showed that the nickel content in bentonite sample was increased after impregnation with the $Ni(NO_3)_2 \cdot 6H_2O$ precursor. Qualitatively, acidity of the catalysts was determined by FTIR showing characteristics for Brønsted and Lewis acids at wavenumbers 1635-1381 cm^{-1}. Surface area analysis results showed an increase in specific surface area after pillarization and impregnation with nickel metal.

Keywords: Catalyst, Bentonite, Zirconium dioxide, Pillarization, Impregnation.

INTRODUCTION

Clay is a natural material constructed from the tetrahedral silica sheet and octahedral alumina. The most important minerals in clays are those that have layered structures and are classified as phyllosilicate. Phyllosilicate is structured lattice silicates which are formed from a series of silica tetrahedral sheets with octahedral alumina bonded due to oxygen atoms used together. Among the most commonly used phyllosilicate clay minerals for making pillared layered solids is the montmorillonite group (bentonite). Montmorillonite attracts a lot of attention as it has the ability to expand (swell) has exchangeable cations and can be intercalated. Montmorillonite is included in the smectite group, having molecular formula $Na_x[Al_{(x-2)}Mg_x(Si_4O_{10})(OH)] \cdot mH_2O$ [1,2].

It is easy to expand nature and its ability to exchange ions through the cations exchange mechanism are potential key points for clay modifications. The modifications inferred include intercalation, which is the replacement of ions between the silicate layers with the cationic polymer in the form of organic compounds or polyhydroxy metals. If polyhydroxy intercalation is performed and continued with calcination, then the process is called pillarization and the resulting material is called pillared clays (PILCs) [3-5].

Clay materials are interesting to be researched because of their chemical and physical properties that can be changed or modified in various ways. In addition, the catalysts in the process of oil cracking that are currently being developed are catalysts with a large pore size in order to be able to crack the heavy oil fraction. The use of clays as catalysts is due to its ability to be modified to form large pore sizes so as to crack long chains of hydrocarbons that cannot enter the zeolite pore. However, some factors such as thermal stability and weak acidity of its in-between layers still need to be overcome. Thus, modifications such as pillarization using metal oxide can be used as an alternative to overcome subdue problems [6-8].

Pillared bentonite has a high porosity obtained through the separation of bentonite sheets with buffer molecules or pillar agents. Preparation is performed by cation exchange of the original bentonite with a part of hydrated polymer or oligo-

This is an open access journal, and articles are distributed under the terms of the Creative Commons Attribution-NonCommercial 4.0 International (CC BY-NC 4.0) License, which allows others to copy and redistribute the material in any medium or format, remix, transform, and build upon the material, as long as appropriate credit is given and the new creations are licensed under the identical terms.

meric metal ion complexes that have been heated and experience dehydration/dehydroxylation generating a pillar arrangement of thermally stable oxide groups of metals. Furthermore, large size pillar agents may form larger channels than zeolites (5-20 Å *versus* 3-11 Å), which make pillared bentonite a suitable catalyst for cracking large molecules such as long-chained hydrocarbons that cannot penetrate the pore system of zeolites [9].

Several investigations have focused on optimizing catalysts synthesis, particularly in the formation of metals and metal oxides dispersed into stable support solids. Zirconium dioxide has been selected in previous studies as a pillaring agent because of its high thermal stability properties and acid properties that play an important role in the cracking mechanism [10]. The acidic character of the pillared bentonite is obtained from Brønsted (proton donor) acid or Lewis acid (electron pair acceptor). Properties of Brønsted acid appear when joined with free protons during the dehydroxylation process of the pillaring agent and the clay sheets, while the Lewis acid properties are associated with the metal oxide of the pillars. The amount and strength of these two properties have strong relation to bentonite type and pillaring agent [11].

Montmorillonite pillarization with ZrO_2 reported by several researches has demonstrated its ability to be applied into high-temperature reactions. Zirconium oxide pillared bentonite exhibits high d(001) value of up to ~ 20 Å and a large surface area (200-300 m^2/g) depending on variable preparation methods [12-14]. Throughout the literature search, the authors had not found any previous research that synthesized nickel metal catalysts embedded in zirconia-pillared bentonite. The objectives of this study, therefore, were to synthesize and determine the physicochemical properties such as basal spacing, skeletal structure, acidity level, specific surface area and morphology of Ni/ZrO_2-bentonite catalyst. The Ni metal was selected as a promoter metal due to its relatively low-cost price, its very strong adsorption ability due to the electrons in *d*-orbitals that are not fully charged and its hydrogenation activity. Nickel metal has been widely applied to hydrocracking reactions either as a single metal or a fusion with other metals embedded in an inert carrier or active catalyst.

EXPERIMENTAL

The materials used in this study were bentonite, $Ni(NO_3)_2 \cdot 6H_2O$ (Merck), $ZrOCl_2 \cdot 8H_2O$ (Merck), ammonia [25 % (v/v)], $AgNO_3$ and distilled water.

Preparation of bentonite: Bentonite was sieved using a 200 mesh sieve, then washed several times with distilled water, vacuum filtrated and dried in an oven at 110-120 ºC. Dry bentonite was crushed until smooth then sieved again using a sieve with mesh size of 200 mesh. The bentonite was later characterized by XRD, FT-IR, XRF, TEM, BET and its surface acidity using gravimetric method with NH_3 vapor.

Synthesis of Ni/ZrO_2-bentonite catalyst: The pillaring solution of oligo-cation zirconia was synthesized by hydrolysis method, where (0.1 M) $ZrOCl_2 \cdot 8H_2O$ solution was refluxed for 2 h at 70 ºC. Then bentonite was added into the oligomer solution slowly and stirred for 24 h at room temperature. Then, the suspension of bentonite zirconia oligo-cation was centrifuged and the obtained precipitate was neutralized with distilled water so that the filtrate is free of chloride ions. The precipitate obtained was dried in an oven at 70 ºC and then crushed and sieved through 200 mesh sieve. Calcination was then performed using the furnace at 400°C for 2 h with a heating rate of 10 ºC/min to obtain ZrO_2-bentonite.

Nickel metal impregnation in ZrO_2-bentonite was performed by the wet impregnation method. A total of 1.4867 g of $Ni(NO_3)_2 \cdot 6H_2O$ was dissolved into 100 mL of distilled water in a round bottomed flask. ZrO_2-bentonite was added and refluxed while being stirred with a magnetic stirrer for 4 h at 80 ºC. The impregnation result was then dried in an oven for 3 h at 110 ºC. Afterwards, the sample was calcined at 500 ºC and purged with N_2 gas with a flow rate of 20 mL/min for 5 h. After calcination, the sample was reduced by purging H_2 gas at 400 ºC and at a flow rate of 20 mL/min for 4 h. The sample was then stored in a desiccator. The Ni/ZrO_2-bentonite catalyst was later characterized by XRD, FT-IR, XRF, TEM, BET and its surface acidity using gravimetric method with NH_3 vapour.

RESULTS AND DISCUSSION

X-ray fluorosence analysis: Table-1 shows the contents of Zr and Ni metals present in Ni/ZrO_2-bentonite samples. The bentonite sample used in this study was detected to contain Ni metal of 0.20 % and did not contain any Zr metal. After pillarization with $ZrOCl_2 \cdot 8H_2O$ precursor and impregnation with $Ni(NO_3)_2 \cdot 6H_2O$, ZrO_2-bentonite sample obtained Zr metal concentration of 52.9 % and Ni metal decreased to 0.04 % [15]. However, an increase in Ni metal concentration was observed, after the impregnation process of Ni/ZrO_2-bentonite sample, to 2.70 % and reduction of Zr metal concentration to 50.9 %. Reduced concentrations of Ni metal in ZrO_2-bentonite and Zr metals samples in Ni/ZrO_2-bentonite samples may be caused by washing and heating at high temperatures (calcination) processes at the pillarization and catalyst impregnation stages.

TABLE-1
Zr AND Ni METAL CONTENTS IN
ZrO_2-BENTONITE AND Ni/ZrO_2-BENTONITE

Sample	Zr (%)	Ni (%)
ZrO_2-bentonite	52.9	0.04
Ni/ZrO_2-bentonite	50.9	2.70

X-ray diffraction analysis: Fig. 1 shows the X-ray diffraction patterns of ZrO_2-bentonite and Ni/ZrO_2-bentonite samples. After the pillarization phase with ZrO_2, the specific peaks of montmorillonite mineral still visible at $2\theta = 19.445°$ (d = 4.561 Å) and $2\theta = 29.197°$ (d = 3.056 Å) [7,14-16].

In previous study, it was found that the clay samples used were montmorillonite minerals with typical peaks in d_{001} at $2\theta = 5.29°$ (d = 16.69 Å) [8]. The typical peak of montmorillonite is still visible but has shifted to angle 2θ smaller than 5º. There is a reflection shift of d_{001} at a low angle associated with an increase of d_{001} as a result of intercalation and pillarization processes. Theoretically, if the pillarization is able to increase the spacing between the silica montmorillonite layers, there will be a shift of the typical peak to the left showing basal spacing

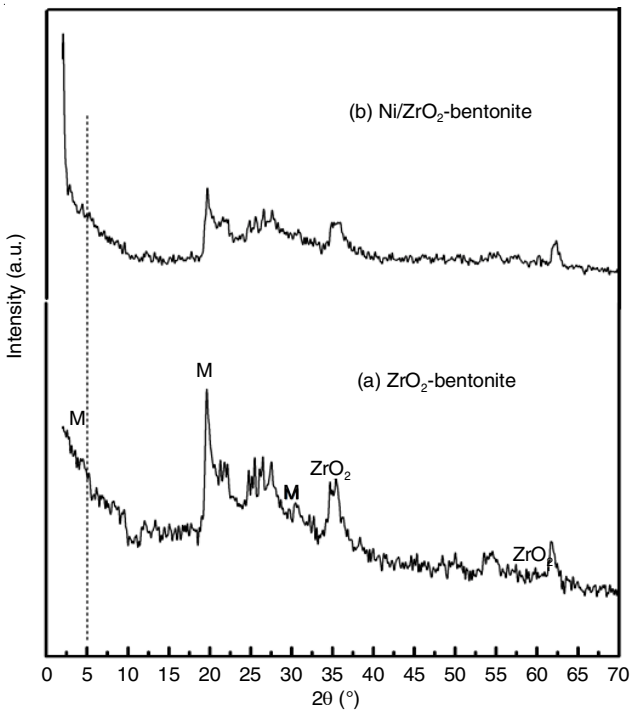

Fig. 1. Diffractogram of (a) ZrO_2-bentonite and (b) Ni/ZrO_2-bentonite

d_{001} [8]. Lower intensity indicates that the thermal treatment and chemical reactions have considerable effects on the montmorillonite structure. Based on previous studies [12] that synthesized metal oxide pillared clays, the data indicate a thermal transformation involving dehydration reaction during the calcination process. The characteristic peaks for ZrO_2 are at 2θ = 34.09º (d = 2.627 Å) and 2θ = 61.65º (d = 1.503 Å).

FTIR analysis: Infrared spectra of ZrO_2-bentonite and Ni/ZrO_2-bentonite minerals were observed at 4000-500 cm^{-1} wavenumbers. Table-2 shows that the key characteristic wavenumbers of several functional groups in bentonite minerals obtained as in previous studies [15].

TABLE-2
WAVENUMBERS AND VIBRATION TYPES IN BENTONITE SAMPLE [Ref. 7,14,15,17-19]

Wavenumber (cm^{-1})	Vibration type
462.92	Bending vibration of Si-O-Si
524.64	Bending vibration of Si-O-Al
879.54	Bending vibration of O-Si-O
918.12	Bending vibration of O-Al-O
1041.56	Stretching vibration of Si-O-Si
1442.75	Stretching vibration of Si-O-Al
1635.64	Bending vibration OH water molecule
3448.72	Stretching vibration OH of Si-OH
3695.51	Stretching vibration OH of Al-OH

Fig. 2 shows the infrared absorption spectra of modified bentonite by means of ZrO_2 pillarization and impregnation with nickel metal. The characteristic absorption band for stretching vibration of OH group of Al-OH has shifted from wavenumber 3695.51 to 3749.62 cm^{-1} in ZrO_2-bentonite and 3626.17 cm^{-1} in Ni/ZrO_2-bentonite which is probably caused by the environmental change due to the bond formation between ZrO_2 pillars and tetrahedral layer. An absorption band at 1041.56 cm^{-1} is a characteristic for Si-O-Si stretching vibration is slightly displaced

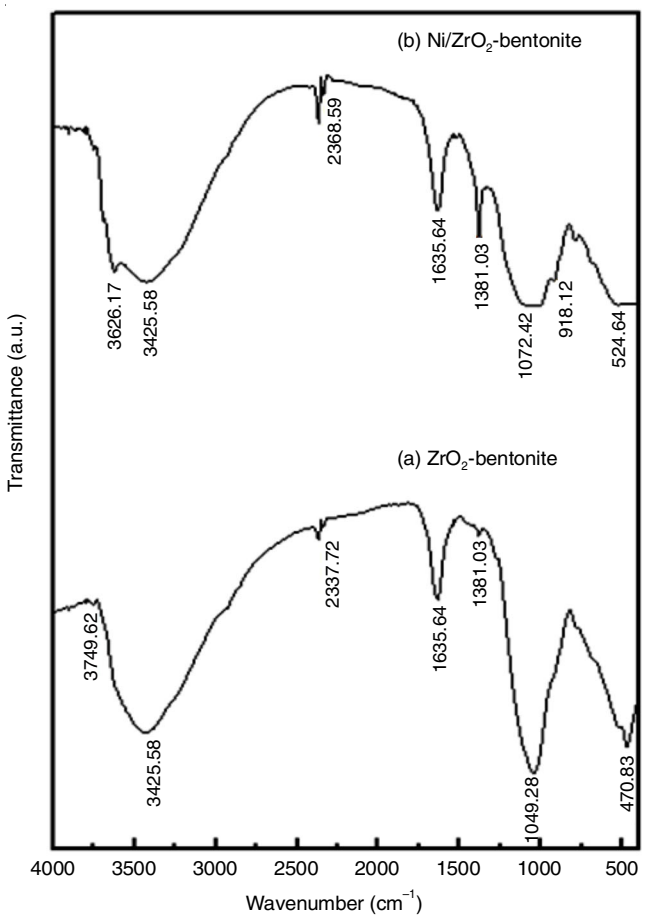

Fig. 2. FTIR spectra of (a) ZrO_2-bentonite and (b) Ni/ZrO_2-bentonite

in ZrO_2-bentonite and Ni/ZrO_2-bentonite samples with wider absorption bands possibly due to the process of pillarization and impregnation of Ni metal.

Fig. 2a shows the absorption bands at wavenumbers that demonstrate the increasingly sharp site of Lewis acid (1635.64 cm^{-1}) which indicates that after the pillarization with ZrO_2, the acidic properties were increasingly strong. One of the reasons as to why this happened is caused by ZrO_2, a transition metal oxide in which Lewis acid properties are derived from zirconium atoms [20]. The absorption band showing the Brønsted acid site at 1442.75 cm^{-1} is less visible indicating the decrease of Brønsted acid strength due to the dehydration in the calcination process at 400 ºC. In Ni/ZrO_2-bentonite sample (Fig. 2b), the absorption band showing Brønsted acid site reappeared after impregnation with Ni metal. The characterization results show that the IR spectra could hardly give a clear indication of the presence of zirconium oxide as a pillar within the interlayer of bentonite [8].

Catalyst acidity test: The acidity test of ZrO_2-bentonite, and Ni/ZrO_2-bentonite samples was performed by ammonia absorption method. Determination of the number of acid sites was done quantitatively by gravimetric technique using the adsorption of ammonia base. The sample acidity (mmol NH_3/g) was determined using the following equation:

$$\text{Acidity (mmol/g)} = \frac{W_3 - W_2}{(W_2 - W_1) \times M} \times 1000$$

where M is the molecular mass of ammonia (17.007 g/mol).

The acidity values of ZrO_2-bentonite and Ni/ZrO_2-bentonite are found to be 4.340 and 7.105 mmol/g, respectively. Based on the determination of acidity above, it appears that the process of pillarization and impregnation had increased the number of acid sites.

In order to find out the distribution of Lewis and Brønsted acid sites on the surface of the catalyst, IR spectra can be useful. Fig. 3 shows the changes that occured in absorption bands with characteristic wavenumbers for Lewis acid sites and Brønsted acid sites after the absorption of ammonia. The Brønsted acid site is formed because of H^+ cation which functions to balance the negative charge of alumina silicate on bentonite [21]. Pillarization significantly increased the acidity of the solids. Lewis's acidity ratio against Brønsted (L/B) is increased by pillarization which means that Lewis's acidity distribution is greater than Brønsted acidity [22].

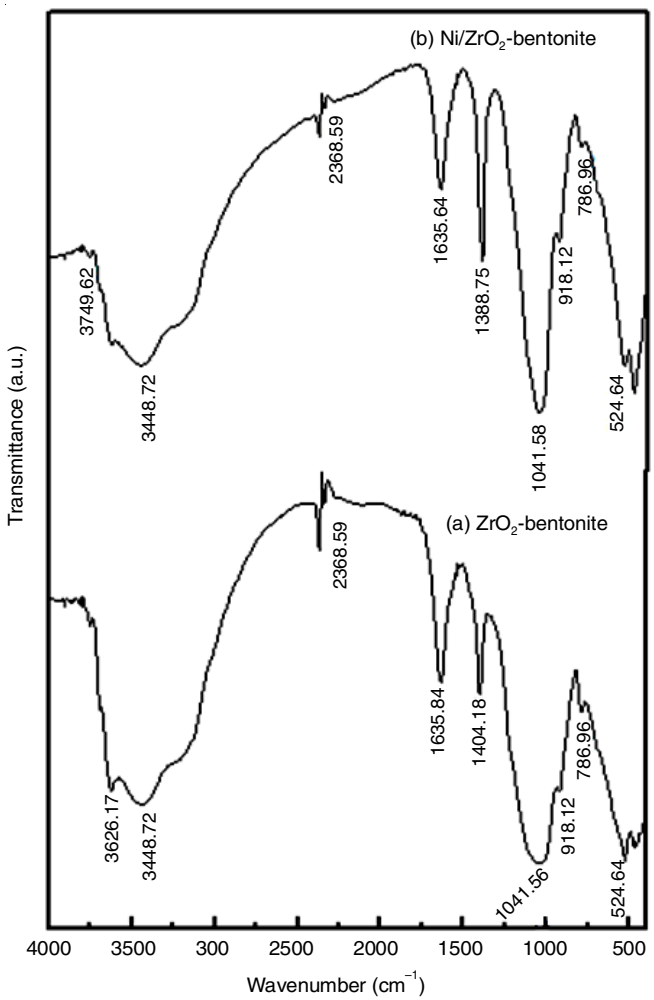

Fig. 3. FTIR spectra of (a) ZrO_2-bentonite and (b) Ni/ZrO_2-bentonite after the absorption of ammonia

The Lewis acid site formed acts as a lone pair electrons acceptor donated by N atoms from ammonia molecules. The bonds that occured between Lewis acid sites and the ammonia molecules were due to the joint use of lone pair electrons from N atoms (covalent coordination bonds). The higher the number of Lewis acid sites, the more ammonia molecules are bonded that result in an increase in the acidity of catalyst.

The band at 1404.18 cm^{-1} showed that the Brønsted acid site reappeared in ZrO_2-bentonite sample after ammonia absorption. Sharpening absorption bands at 1388.75 cm^{-1} after absorption of ammonia in Ni/ZrO_2-bentonite sample showed the strength of Brønsted acid site. The presence of H^+ cation in bentonite will interact with NH_3 gas adsorbed on the surface of bentonite and forms ammonium ion (NH_4^+).

Surface area and porosity analysis: Surface area, pore diameter and pore volume measurements were determined by BET surface area analyzer (SAA) instrument. Specific surface area, pore diameter and pore volume of bentonite obtained in the previous study were 27.385 m^2/g, 10.16 Å and 0.139 cc/g, respectively. This surface area experienced a significant increase to 89.115 m^2/g after bentonite was modified by pillarization with ZrO_2 (Table-3). Pillarization causes an increase spacing between layers of silica due to the insertion process of active metal components into the space between layers of silica in bentonite. Pillarization also lead to the formation of house of cards structure through the formation of new pores into micropores, whilst the card structure caused the pore size to become mesoporous [14]. Table-3 also shows an increase in the specific surface area of ZrO_2 pillared bentonite after impregnation with nickel metal to 99.071 m^2/g. This increase in surface area can be attributed to the formation of new pores due to the accumulation of nickel metal particles in open pores which also directly cause a decrease in pore diameter and pore volume.

TABLE-3
RESULT OF SURFACE AREA, PORE DIAMETER AND PORE VOLUME

Sample	Surface area (m^2/g)	Pore diameter (Å)	Pore volume (cc/g)
ZrO_2-bentonite	89.115	49.77	0.222
Ni/ZrO_2-bentonite	99.071	20.29	0.100

The isotherm adsorption-desorption pattern of N_2 gas on ZrO_2-bentonite and Ni/ZrO_2-bentonite samples is shown in Fig. 4. Based on the isotherm adsorption according to BDDT classification, the isotherm patterns of both samples fall under type IV, showing that the adsorption of solids and pore diameter are greater than the micropore (the formation of mesoporous solids) which is characterized by the hysteresis loop. The pattern of isotherm adsorption-desorption of bentonite samples used in this study also fall under type IV. The type IV isotherm patterns have four types of hysteresis loop according to IUPAC. The hysteresis loops of bentonite, ZrO_2-bentonite and Ni/ZrO_2-bentonite, are H3 hysteresis loop type indicating the presence of pores with a narrow slit structure [22].

TEM analysis: A morphological analysis showing changes in the interlayers of bentonite, ZrO_2-pillared bentonite and ZrO_2-bentonite embedded with 1 % Ni metal are shown in Fig. 5. The parallel lines showing the layered structure of bentonite are increasingly apparent after the pillarization stage with ZrO_2 (Fig. 5b). This demonstrates that the successful insertion of zirconium metal oxides as pillaring agents in the silica interlayers of bentonite. The same is also shown in the observation of the specific surface area that increased significantly after the bentonite pillarization stage as shown by the BET data.

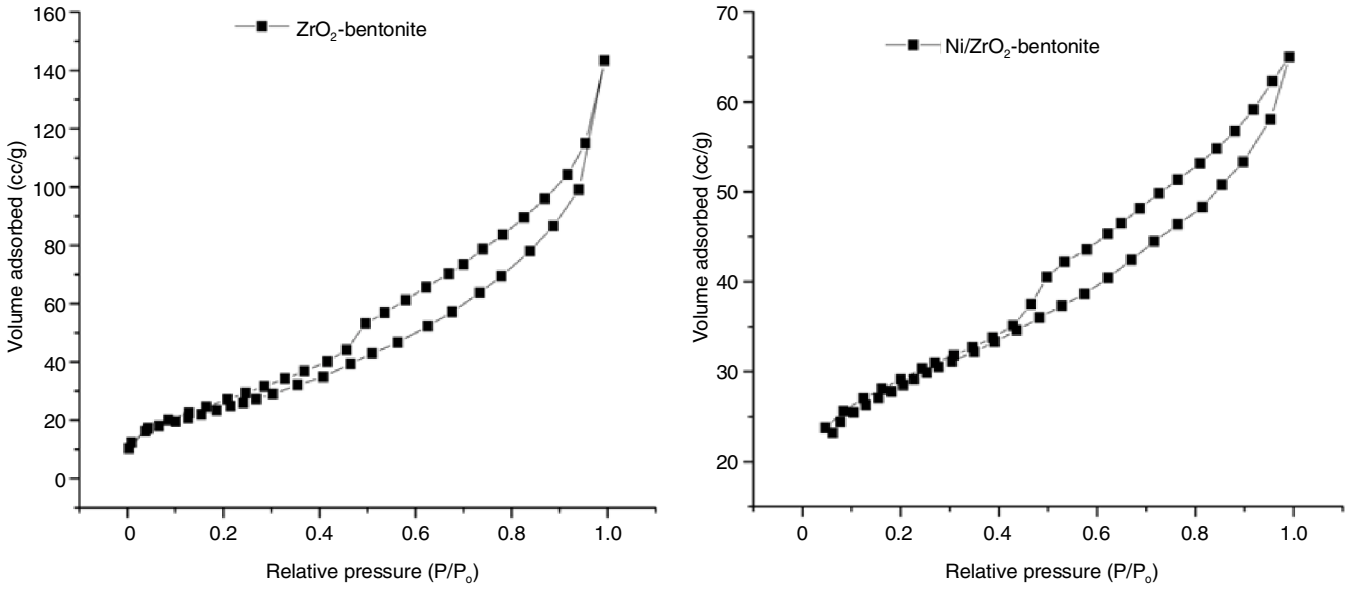

Fig. 4. Isotherm adsorption-desorption patterns ofZrO_2-bentonite and Ni/ZrO_2-bentonite

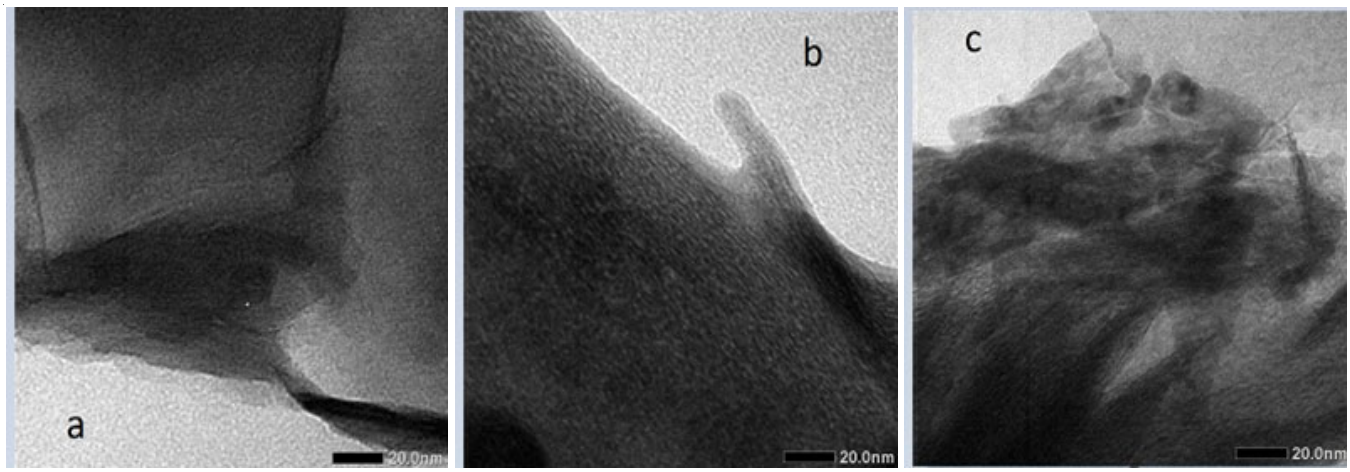

Fig. 5. Morphology of (a) bentonite (b) ZrO_2-bentonite and (c) Ni/ZrO_2-bentonite

Fig. 5c shows the increasing number of black spots on the surface of ZrO_2 pillared bentonite which is thought to be the accumulation of embedded Ni metals that consequentlyform a new pores. Nickel metal exposure resulted in a increase in the specific surface area of ZrO_2 pillared bentonite (BET data), and did not cause collapse and breakage of pillars on the bentonite cross-section as shown in the XRD where the typical peak of d_{001} was still formed and a reflection shift occured at the lower angle associated with increase of basal spacing d_{001}.

Conclusion

There is a reflection shift of d_{001} at a low angle associated with an increase of d_{001} as a result of intercalation and pillarization processes. The Ni metal impregnation stage does not cause the collapse of the pillar, displayed by the still-typical peak d_{001} at the lower angle. The catalyst synthesis produced a catalyst with increasing acid properties proven through the acidity test involving absorption of ammonia. There is an increase in the specific surface area, after bentonite pillarization and nickel metal impregnation step.

ACKNOWLEDGEMENTS

The financial support by the Ministery of research, Technology and Higher Education, Republic of Indonesia under multi years PTUPT 2018 Research Grant is gratefully acknowledged.

CONFLICT OF INTEREST

The authors declare that there is no conflict of interests regarding the publication of this article.

REFERENCES

1. T.J. Pinnavaia, *Science*, **220**, 365 (1983); https://doi.org/10.1126/science.220.4595.365.
2. F. Uddin, *Metall. Mater. Trans. A*, **39**, 2804 (2008); https://doi.org/10.1007/s11661-008-9603-5.
3. A. De-Stefanis and A.G. Tomlinson, *Catal. Today*, **114**, 126 (2006); https://doi.org/10.1016/j.cattod.2006.01.019.
4. A. Gil, S.A. Korili, R. Trujillano and M.A. Vicente, *Appl. Clay Sci.*, **53**, 97 (2011); https://doi.org/10.1016/j.clay.2010.09.018.

5. A.G. Tomlinson, *J. Porous Mater.*, **5**, 259 (1998); https://doi.org/10.1023/A:1009686322154.
6. F. Kooli and W. Jones, *Chem. Mater.*, **9**, 2913 (1997); https://doi.org/10.1021/cm970254s.
7. K. Wijaya, A.S. Pratiwi and S. Sudiono, *Indonesian J. Chem.*, **2**, 20 (2002).
8. K. Wijaya, E. Sugiharto and I. Mudatsir, *Indonesian J. Chem.*, **4**, 33 (2004).
9. Z. Ding, J.T. Kloprogge, R.L. Frost, G.Q. Lu and H.Y. Zhu, *J. Porous Mater.*, **8**, 273 (2001); https://doi.org/10.1023/A:1013113030912.
10. S. Moreno, S.K. Kou, K. Molina and G. Poncelet, *J. Catal.*, **182**, 174 (1999); https://doi.org/10.1006/jcat.1998.2349.
11. M.E. Gyftopoulou, M. Millan, A.V. Bridgwater, D. Dugwell, R. Kandiyoti and J.A. Hriljac, *Appl. Catal. A Gen.*, **282**, 205 (2005); https://doi.org/10.1016/j.apcata.2004.12.012.
12. A. Gil, A. Vicente and M. Gandia, *Micropor. Mesopor. Mater.*, **34**, 115 (2000); https://doi.org/10.1016/S1387-1811(99)00166-3.
13. J.T. Kloprogge, *J. Porous Mater.*, **5**, 5 (1998); https://doi.org/10.1023/A:1009625913781.
14. M.E.R. Jalil, M. Baschini and K. Sapag, *Materials*, **10**, 1345 (2017); https://doi.org/10.3390/ma10121345.
15. J. Ruslan, Hardi andM. Mirzan, Synthesis and Characterization of Sulfated Zirconia Pillared clay as Cracking Catalyst, Yogyakarta State University, Indonesia, Proceedings of The National Chemistry Seminar, p. 325 (2017).
16. Y. Utubira and K. Wijaya, *Int. J. Chemtech Res.*, **9**, 475 (2016).
17. K.A. Carrado, L. Xu, R. Csencsits and J.V. Muntean, *Chem. Mater.*, **13**, 3766 (2001); https://doi.org/10.1021/cm010104o.
18. J. Madejova, *Vib. Spectrosc.*, **31**, 1 (2003); https://doi.org/10.1016/S0924-2031(02)00065-6.
19. W. Xue, H. He, J. Zhu and P. Yuan, *Spectrochim. Acta A Mol. Biomol. Spectrosc.*, **67**, 1030 (2007); https://doi.org/10.1016/j.saa.2006.09.024.
20. D.A. Ward and E.I. Ko, *J. Catal.*, **150**, 18 (1994); https://doi.org/10.1006/jcat.1994.1319.
21. S.M.R. Kou and S. Mendioroz, *Clays Clay Miner.*, **48**, 528 (2000); https://doi.org/10.1346/CCMN.2000.0480505.
22. I. Fatimah, Ph.D. Dissertation of Chemistry, Faculty of Mathematics and Natural Sciences, Gadjah Mada University, Yogyakarta, Indonesia (2010).